Identification of Various Frequency Response Functions for Levitating Rotor System using Active Magnetic Bearings

Michael Kreutz[1,2], Johannes Maierhofer[1], Thomas Thümmel[1], and Daniel J. Rixen[1]

[1] Chair of Applied Mechanics, Technical University of Munich, Garching, Germany
[2] m.kreutz@tum.de

Abstract

Frequency response functions (FRFs) of rotor systems can be used as indicator functions for condition monitoring. Component-wise FRFs are of high interest to locate errors in the fault case. To enable continuous monitoring, measurements should be taken during operation.

This contribution shows methods of using active magnetic bearings (AMBs) for determining different FRFs of a rotor system. The AMBs are used as combined sensors and actuators and at the same time as support for the rotor. Two different types of FRFs, namely for the free rotor and the supported/bounded system dynamics can be determined from a single experiment. This procedure does not need any change in the assembly, because the AMBs are simultaneously used as bearing and exciter. Using the ground reaction force of the magnetic bearings gives the free rotor's FRF. The supported system's FRF is determined by considering the excitation force only.

As show-case, an academic rotor test rig is used with and without rotation to show the general feasibility of the method. To evaluate and interpret the results of the experiments, a numerical model of the rotor using finite-element formulations is used.

1 Introduction

Condition monitoring compares a rotor system's actual behavior with a desired or normal behavior using indicators to detect faults. In [16], multiple rotor faults are described. Indicator functions can be for example frequency response functions (FRFs) or modal parameters. Mechanical FRFs $\boldsymbol{H}(\omega)$ are defined as the linear relationship between harmonic forces $\boldsymbol{F}(\omega)$ and harmonic responses $\boldsymbol{X}(\omega)$ (displacement, velocity, acceleration) which depend on the excitation frequency ω, cf. [2].

$$\boldsymbol{X}(\omega) = \boldsymbol{H}(\omega)\,\boldsymbol{F}(\omega) \tag{1}$$

In a simulation model, it is easy to obtain the FRFs. For a symmetric rotor, considering gyroscopic effects, the FRFs for a rotational speed Ω can be obtained by

$$\boldsymbol{H}(\omega) \;=\; \left(-\omega^2\boldsymbol{M} \;+\; i\omega\left(\boldsymbol{C} + \boldsymbol{G}\left(\Omega\right)\right) + \boldsymbol{K}\right)^{-1} \tag{2}$$

with the system's mass, damping, gyroscopic and stiffness matrix $\boldsymbol{M}, \boldsymbol{C}, \boldsymbol{G}, \boldsymbol{K}$ respectively.

For an experimental determination, there exist a number of algorithms, based on fast Fourier transforms, that estimate the FRF from a set of given input (force) to output (response) time-signals. Determining the FRFs is the first part of experimental modal analysis (EMA). Measuring the FRFs of rotating systems is a special challenge.

Strategies to measure the FRFs of rotating systems have been proposed in the BRITE/-MARS project [4], also given in related items [3]. In these publications, active magnetic bearings (AMBs) are used as excitation system additional to existing support in ball bearings. In [6],

an approach for combining the AMB's control system with a MIMO identification procedure to obtain a state-space model through the system's FRFs is given for systems with real poles. In [5], a method to combine the magnetic bearing's support with an additional excitation is given. This is similar to the method applied in this contribution. Here, we want to use a simple implementation of standard MIMO excitation signal, as e.g. burst random excitation, which can be found in text books about EMA, for example in [2, p. 323ff]. We also want to give an intuitive interpretation of the results, to understand how AMBs can be used to get different FRFs of one system in a single experiment.

In [12], an approach of using AMBs to perform EMA of the supported rotor system using an external commercial modal analysis system was shown for the levitating, but non-rotating rotor.

In order to measure the FRFs of a system, typically, its operation must be stopped. The system must be instrumented by exciters and sensors. The system is excited and from the resulting time-data, it is possible to determine the FRFs. Stopping the system's operation and performing the tests takes a lot of time and effort, so this is not feasible for condition monitoring. In this contribution, the AMBs are used as combined exciters and sensors, while still being used as bearings. This enables to measure the FRF of the rotor system during operation, without the need to stop its operation. The excitation force and the total force in the bearing is estimated by a linear current-force relationship. With this, it is possible to determine the FRFs of the supported system and of the free rotor in a single measurement run. Thus, using FRFs for a continuous condition monitoring of the rotor system is enabled. The availability of the supported system's FRF and free rotor's FRF is especially useful for localizing faults in the rotor system as the bearing effects can be separated from the rotor effects in the different FRFs.

Here, the test rig's control system is used for measuring the necessary data, without the need for an additional modal analysis system. The excitation is applied via the bearings, using an additional excitation current that is added to the AMB's controller current. The combination of the excitation and bearing task in the magnetic bearing enables to measure FRFs of different theoretical system configurations in a single experiment but by considering different force signals. Namely: Considering only the additional excitation force gives the supported rotor system's FRFs. Considering the total force, comprised of contributions from the controller and from the additional excitation, gives the free rotor's FRF.

In this contribution, the approach will be applied to an academic test rig with and without rotation. First, the test rig and a simulation model of the test rig is explained. Then results of applying the method to a non-rotating system are given and interpreted. The method is then also applied to a rotating system, which shows its feasibility. In the end, a short summary of the contribution is given.

2 Test Rig and Simulation

The magnetic bearing test rig at the Chair of Applied Mechanics of the Technical University of Munich will be used as an example of a levitating rotor in magnetic bearings. In fig. 1, the test rig with its components is given. The test rig is also described in [8, 10]. The rotor is supported in active magnetic bearings and can be driven by a servo motor which is coupled to the rotor via a double cardan joint. A mass disc and two bearing journals are attached to the rotor. Displacements are measured in planes on the front and back plate of each magnetic bearing via eddy current sensors. Measuring the acceleration by adding acceleration sensors to the rotor is not feasible, because the system should be able to rotate. Compared to the test

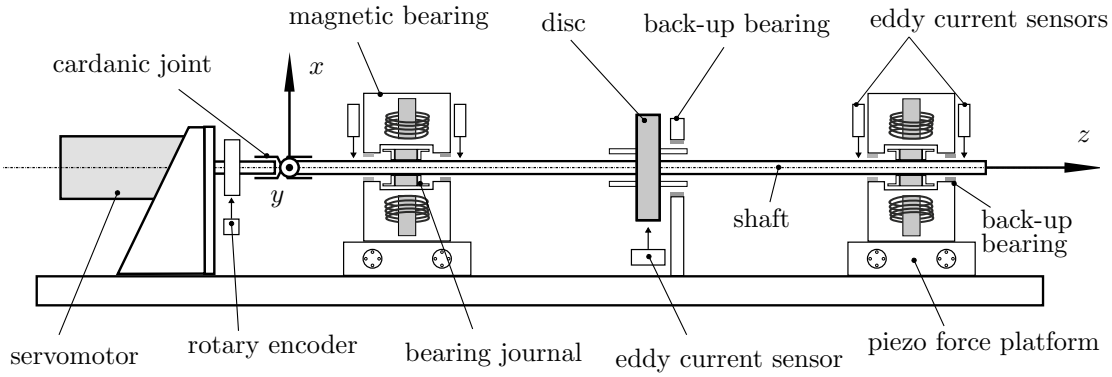

Figure 1: Schematic view of the magnetic bearing test rig, see also [10].

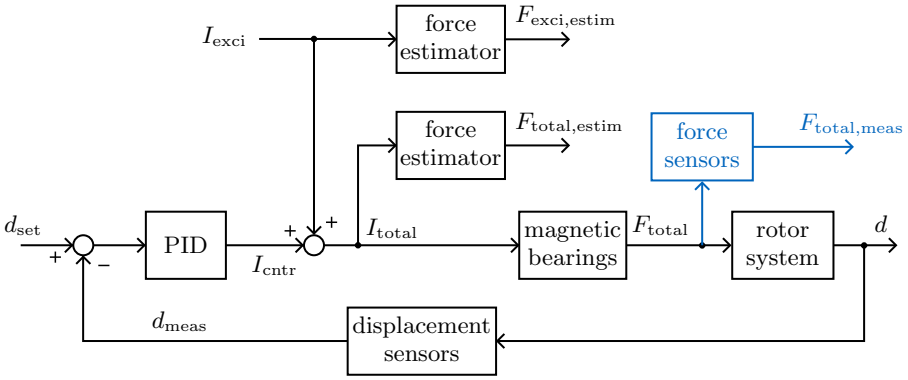

Figure 2: Control scheme including additional excitation.

rig configuration in [10], the test rig has been improved by applying additional force-torque sensors (piezo force platform Kistler 9129AA) underneath the magnetic bearings. They give an accurate reading of the magnetic bearing ground force, which corresponds to the total force of the bearing. It is used later for a comparison with the results using a force estimation for the total force.

The position of the rotor in the magnetic bearings is controlled by a PID controller, which uses the position error with the measured displacement d_{meas} as input signal and a controller current I_{cntr} as output. The PID controllers are implemented separately for each direction. A control scheme of the system is given in fig. 2. Only small vibrations inside the bearing are assumed, so that the magnetic force law is not influenced by the position in this example. An additional excitation current I_{exci} can be applied to the magnetic bearings by adding it to the controller current. The force resulting from the excitation current I_{exci} cannot be measured directly. The measured force $F_{\text{total,meas}}$ contains both contributions from the controller current I_{cntr} and the excitation current I_{exci}, which cannot be easily separated:

$$F_{\text{meas}} = f(\, I_{\text{cntr}} + I_{\text{exci}},\, \dots\,). \tag{3}$$

An ideal behavior of the force sensors is assumed ($F_{\text{total}} \approx F_{\text{total,meas}}$). In order to be able

to separate the forces, we assume a linear relationship between the applied current and the resulting force.

$$F = k_i I, \qquad \text{with } k_i = \frac{\sqrt{2}}{4} \cdot 50 \,\frac{\mathrm{N}}{\mathrm{A}} \approx 18 \,\frac{\mathrm{N}}{\mathrm{A}} \tag{4}$$

The factor k_i was determined at the chair in a similar test rig to [11]. The bias current is $I_b = 2.5\,\mathrm{A}$. The magnetic bearings are actuated in a differential driving mode, e.g. [14, p.125]. In eq. (4), the current I is split in current between opposing coils, where one coil is actuated with $I_{\mathrm{coil},1} = I_b + I_{\mathrm{total}}/2$ and the opposing coil with $I_{\mathrm{coil},2} = I_b - I_{\mathrm{total}}/2$.

In general, the magnetic bearing force law is non-linear, but in special cases, e.g. for a low current and small displacements, a linear relationship may be assumed. The non-linearity between displacement, current and force for this magnetic bearing was investigated in [11].

The excitation and total force are estimated from eq. (4)

$$F_{\mathrm{exci,estim}} = k_i I_{\mathrm{exci}}, \qquad F_{\mathrm{total,estim}} = k_i I_{\mathrm{total}}. \tag{5}$$

They should be used to calculate the FRFs of the assembled system and the free rotor in this contribution. The force $F_{\mathrm{total,meas}}$ is directly measured by the force platforms. The results using the measured force are used as comparison to the results using the estimated total force. This is possible in the academic test rig. In an industrial application adding force measurement adds a lot of cost and complexity and is often not possible due to space restrictions.

2.1 Measurement Setup

In the experiments, FRF-measurement is performed by using the active magnetic bearings as exciters. The experiment uses burst random excitation in x-direction for both AMBs, which consists of 0.5 s excitation using band-limited noise (limited to 250 Hz, amplitude 1.6 A). This is followed by 1.548 s pause. For information about burst random excitation, see [2, p. 338]. As independent burst random excitations are applied on both AMBs, this is a multiple input multiple output (MIMO) identification procedure. It is important for MIMO identification, that the excitation signals are uncorrelated. The measurement duration is 204.8 s with a sampling rate of 10 kHz.

The resulting FRFs are calculated from the time data of force and displacement signals by using algorithms included in ABRAVIBE [1], which is a companion software for the text book [2]. The standard H_1-estimator is used, because it is widely spread and easily applicable to MIMO identification. A Hanning window (2.048 s long) with 67 % overlap is used.

2.2 Simulation

To help the interpretation of the experimental results, a numerical model of the test rig is used. The numerical model is built using the open-source rotor simulation toolbox AMrotor, cf. [7, 9]. A model of the system has been built in [8]. The model of the free rotor has been validated using a commercial modal analysis system with impact excitation of the free rotor, disassembled from the test rig. The magnetic bearings are represented as simple linear spring-damper elements with $k_{\mathrm{AMB}} = 1.3 \times 10^5\,\mathrm{N/m}$ and $d_{\mathrm{AMB}} = 90\,\mathrm{N\,s/m}$. The magnetic bearing forces are assumed to be applied to the middle point in each AMB. The free system is the rotor without added spring-damper-element. The assembled system is the rotor including the spring-damper element as basic model of the magnetic bearings.

3 Non-Rotating System

The experimental results for the non-rotating system are obtained in a single measurement and are validated by comparison with simulation results.

3.1 FRF of Rotor in AMBs Using Additional Excitation Force

In a first step, only the additional excitation force on the AMBs is considered as an input to the FRF calculation algorithm. The excitation force is estimated from the linear static relationship in eq. (5).

Figure 3 shows a simple model of the resulting system. As only the additional force is considered, the bearings forces are considered as internal forces and thus are included in the dynamic FRF. The abbreviation *supp* is used for the *supported* system.

$$\boldsymbol{X}(\omega) = \boldsymbol{H}_{\text{supp}}(\omega)\, \boldsymbol{F}_{\text{exci}}(\omega) \tag{6}$$

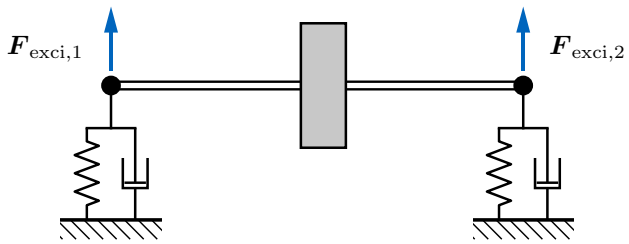

Figure 3: Model of the identified system using F_{exci} as input signal.

Figure 4 shows the experimental results for the FRF using only the additional excitation force and compares them with the results from the numerical simulation for the rotor in elastic bearings. It shows the FRF between excitation at the right AMB and the response at the rightmost eddy current sensor. The excitation and response positions are very close, so a behavior similar to a driving point FRF is expected. The experimental and simulation results are clearly similar. The coherence of the experimental FRF is shown in orange. It starts to fall at around 200 Hz, because of using band-limited noise with a cut-off frequency of 250 Hz as part of the burst random excitation.

The first peak at 16.6 Hz agrees very well in simulation and experiment. The peaks at around 60 Hz are due to the magnetic bearing influence. For these, the simulated eigenfrequencies are lower, than in the experiment. This can be explained by an error in the spring-damper-parameters, that represent the AMBs in the simulation. For the peaks above 100 Hz the simulation deviates from the experiment. They are hardly influenced by the spring-damper parameters in the simulation, but are rather influenced by the stiffness, damping and mass of the rotor itself. Especially the correct damping in the rotor must be determined more accurately. A more accurate model of the rotor should improve the results, e.g. by model updating procedures.

There is an offset in the amplitude between the experimental and simulation results. This is due to an error in the current-force-factor k_i. Additional deformation is brought to the test rig by the force platform itself.

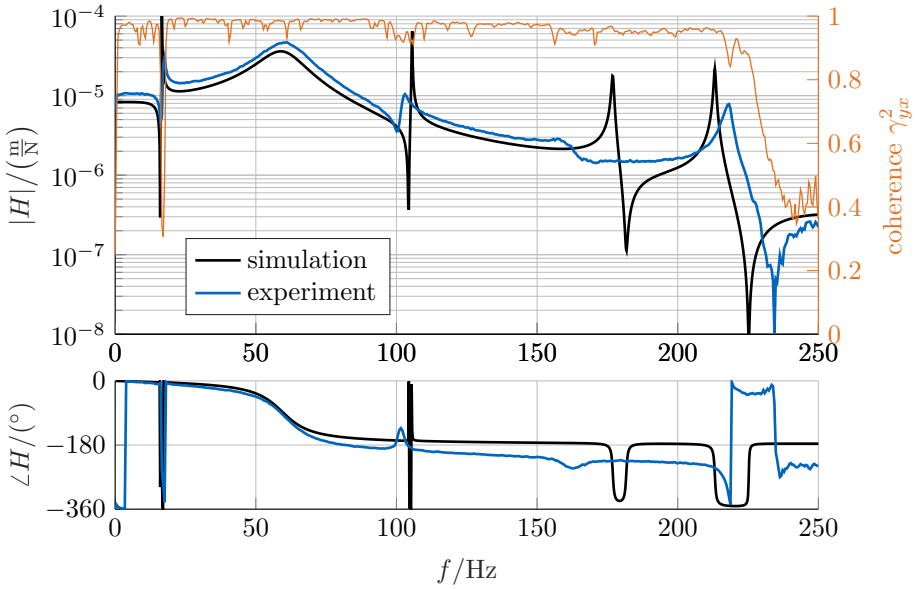

Figure 4: FRF H_{supp} of the rotor supported in magnetic bearings (using only excitation force), non-rotating.

The phase of the FRF shows a similar behavior in simulation and experiment. As expected, the phase falls $-180°$ for resonances and rises $180°$ at anti-resonances. The phase of the experimental FRF falls down linearly. This is due to effects in the current amplifier, mainly time-delay. These effects are not compensated in the static force estimation (using k_i), so they show up here.

Both curves show anti-resonances close to the resonance frequencies. This means, that the points for excitation or response measurement are very close to vibration nodes. This is due to considering the points at the AMB. The AMB's controller tries to minimize the displacement, because it acts as a bearing. Naturally, the vibration nodes will be close to the bearing. The close vicinity of the excitation and measurement points to the bearing is a disadvantage of the method and means a bad observability and controllability of these points. The stiffer the AMBs act, the worse the problem gets.

This also means, that the resulting FRFs are very sensitive to the exact positioning of the sensors, as they are close to the vibration nodes. Small mistakes in the position have a rather large influence on the measured FRFs. So, an inherent problem of the method is, that the excitation position is very close to the vibration nodes.

This experiment showed the measurement of the supported rotor FRF, using a force estimation using only the additional excitation current.

3.2 FRF of Free Rotor Using Total Force

In this section the total force of the AMB is considered for the FRF calculation algorithm. Figure 5 shows the rotor that is cut free from the bearings. The total force is estimated from eq. (5) and measured by the force platform. It is the force that acts between the ground and the magnetic bearings. It includes the additional excitation force and the controller force. The

controller force can be seen as the reaction force of the bearings. It is now assumed to be part of the external excitation and the bearings are therefore no longer part of the characterized system. So only the rotor without the bearings remains, i.e. the free rotor.

$$\boldsymbol{X}(\omega) = \boldsymbol{H}_{\text{free}}(\omega)\, \boldsymbol{F}_{\text{total}}(\omega) \tag{7}$$

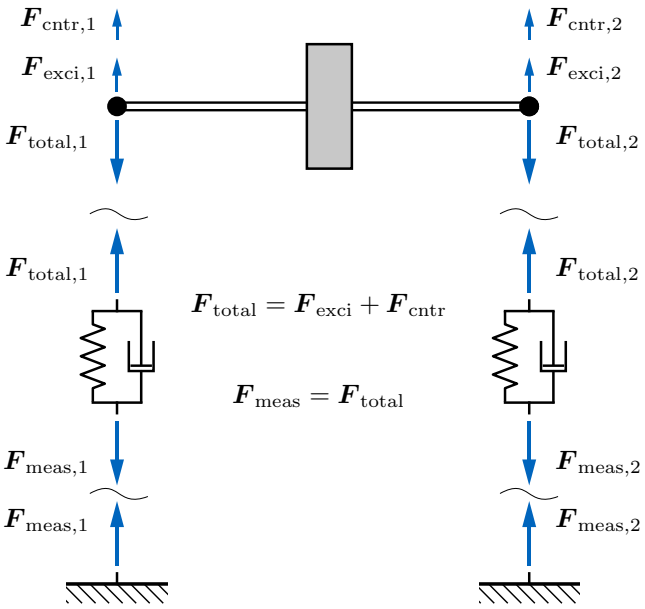

Figure 5: Model of the identified system using the total force F_{total} as input signal.

For this example the estimated total force should be used and compared with the results from the measured total force. There are several methods to determine the total force. In [5], some possibilities are given, that are shortly repeated here:

- Measuring the force between the AMB and the ground. It is suggested to consider the inertia of the AMB. Here, we neglect this influence, as the force platform is assumed to be rigid.
- Measuring the magnetic flux density B using a Hall-sensor in the AMB and estimating the force using the area of the electromagnet and the magnetic permeability constant. This method enables the magnetic bearing to measure the total force, without using additional force sensors, making the AMB a self-sensing active component.
- Estimating the force from a model. This can be a model, which has been parameterized experimentally or which used theoretical knowledge about the AMBs from an electromagnetic simulation model. Here, the force is estimated using a linear static current-force relationship, eq. (5).

Figure 6 shows the results for the experimental FRF using the total force between the right magnetic bearing and the rightmost eddy current sensor. It shows the amplitude and angle of H_{free} and its coherence for the experimental results. This experimental FRF is obtained by using different signals from the same experiment as in previous section 3.1. The curves

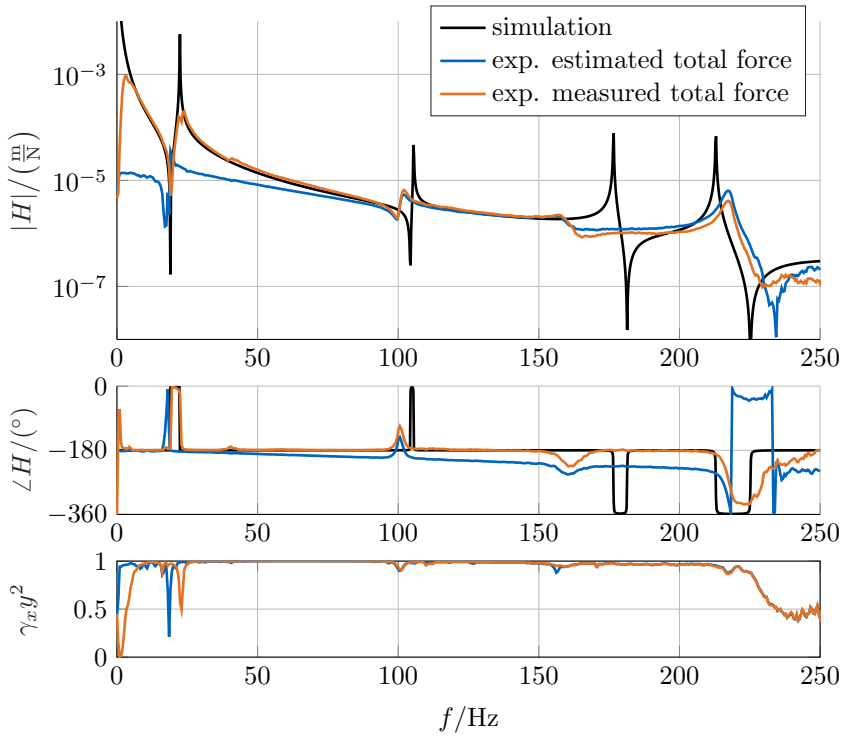

Figure 6: FRF H_{free} of the free rotor (using the total force), non-rotating, with coherence.

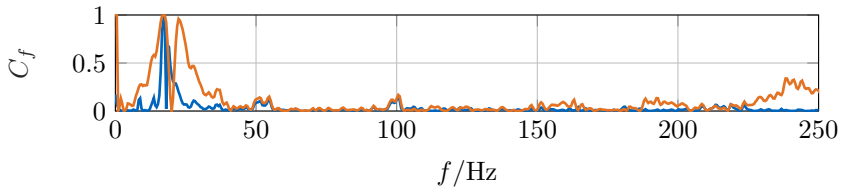

Figure 7: Ordinary coherence between the two input signals (total force).

exp. measured total force use the force that is directly measured by the force platforms F_{meas}. The curves *exp. estimated force* use the force that is estimated from the total electric current $F_{\text{est,total}} = k_i \cdot I_{\text{total}}$. It is compared to the simulation results for the free rotor system.

For the FRF of a free system, one expects to see the effect of the rigid body modes, i.e. the amplitude starts at infinity, $|H\,(f \to 0)| \to \infty$. This can be clearly seen in the simulation results. In the experimental results, this is less obvious. For the measured force FRF the amplitude agrees after about 6 Hz. For lower frequencies the amplitude does not match. In order to go to infinity, the FFT of the force must go to zero, which is not possible in practice, as the force signal is then primarily dominated by noise. The amplitude above 6 Hz and outside of the resonance points agrees very well, using the force platforms.

The FRF from the estimated force approaches the correct amplitudes only at approx. 100 Hz. Before that, there is a distinct error, that is due to the insufficient force estimation for high

currents, which are present at lower frequencies. The solution using the estimated force deviates from the measured force. The real current I_{total} is not measured directly. But it is assumed that the behavior of the electrical system is ideal, i.e. a desired current is perfectly executed. In reality, this does not hold, which can be seen by the deviation of the FRFs in the frequency region up until 90 Hz, where large currents and thus forces are requested. The system could be improved by adding a system for current measurement. Current measurement systems are cheaper and more easily available, than the applied force platforms. Implementing the measurement method in a practical application would only use a force estimation by a measured current, as this saves costs compared to a direct force measurement.

As in the previous section, the simulation model agrees very well with the experimental result for the measured total force in the first peak and is stiffer than the experimental system for eigenfrequencies over 100 Hz.

At the position of the peaks, the amplitudes do not agree, because of inaccuracies in the rotor model (damping) and also because the free rotor has vibration nodes close to the measurement position, which makes the system sensitive to small positioning errors. In contrast to the previous section, this is not an inherent problem of the method, but rather the case for this special rotor system, which has concentrated mass at the bearing journal while the rest of the rotor is rather slim.

Compared to the previous section, there is no eigenfrequency at around 60 Hz, which was found from identification of the rotor with supports in the previous section 3.1.

The phase of the FRFs show a similar behavior between simulation and experiment.

The coherence has small dips at resonance points.This is especially relevant for the first peak. In fig. 7 the ordinary coherence (correlation) between the input signals is shown. The controller force is dominant when there is large displacement that has to be controlled. At resonance frequencies of the supported system the displacement is large and thus strongly influences the total force and thus its correlation. A high correlation of the input signals can cause problems in the FRF calculation due to the poor conditioning of the problem, cf. [2, p. 327].

Another effect that can negatively influence the results is internal feedback in the measured system. This can lead to biased FRFs, cf. [3]. In this magnetic bearings, the displacement within the magnetic bearing directly influences the magnetic force. This influence was neglected in this contribution.

3.3 Interim Conclusion

It has been shown, that it is possible to measure the FRF of the supported rotor system and of the free rotor in a single measurement run. For a better agreement of experimental and simulation results, the numerical model should be updated. Particularly, the damping is not well represented. The supported system's FRFs were experimentally determined by estimating the excitation force from the current. The results agree well. The free rotor's FRFs were determined by considering the total force. The experimental results using the force estimation do not represent well the amplitude for small frequencies. There, the estimation is insufficient, because of high currents. However, the overall behavior agrees well with simulation and experimental results using measured force.

The results for the FRFs using only force estimation showed differences in amplitude compared to simulation results or to measured force FRFs. In continuous condition monitoring the FRFs (indicator function) of a rotating machine are continuously compared to previous FRFs. So, only differences in the FRFs are important, while the exact amplitude is of less importance, which implies the suitability of the presented FRF aquisition using estimated forces.

4 Rotating System – FRF of Free Rotor

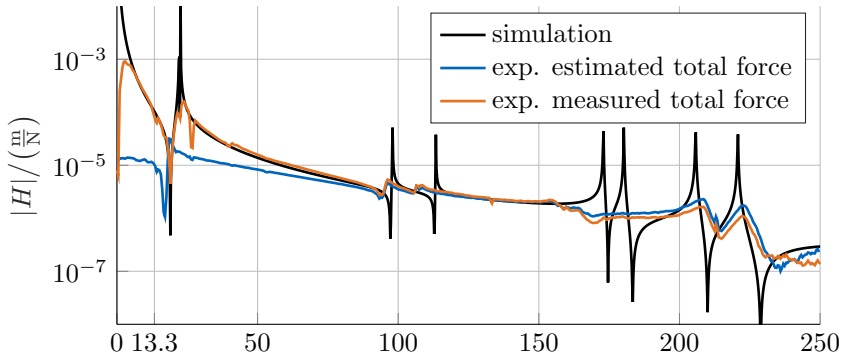

Figure 8: FRF amplitude $|H_{\text{free}}|$ of the free rotor (using total force) for 800 rpm

In this section, an example of applying the measurement method to obtain the free rotor's FRF on the rotating system is shortly displayed.

As given in eq. (2), in simulation the FRF of a symmetric rotor at a given speed can be easily obtained from the system matrices. However, experimental measurement of the FRFs for the rotating system are hard to get. Especially the FRF of the free rotor cannot be obtained by usual EMA techniques, like e.g. impact testing.

Using the technique shown in this contribution, the rotor is excited in its magnetic bearings and the total force is used for FRF-estimation. Figure 8 shows the determined FRFs in simulation and from the experiment for a rotational speed of 800 rpm $\approx$ 13.3/s. Two results from the experiment are shown.

The results are similar to fig. 6. Due to the rotational speed, gyroscopic effects occur, which split the eigenfrequencies. This can be seen in occuring double peaks for the tilting modes. At the frequency of the rotation, which is marked in the figure, the FRF with the measured force is has a small dip. At frequency 2Ω, there is a disturbance from the rotational speed, which is greater in magnitude. So, the FRFs of the rotating system can be determined accurately with little disturbance from the rotation.

Figure 9 gives a summary of the experimentally determined FRFs. Each sub-figure shows the results from one measurement run, for 0 rpm and 800 rpm respectively. This clearly shows the difference between the supported system's and free rotor's FRFs, where the rigid body modes are apparent at small frequencies for the free system and the distinct peak at around 60 Hz only appears in the supported system. By comparing the left and right parts of fig. 9, the splitting of eigenfrequencies with rotation can be seen.

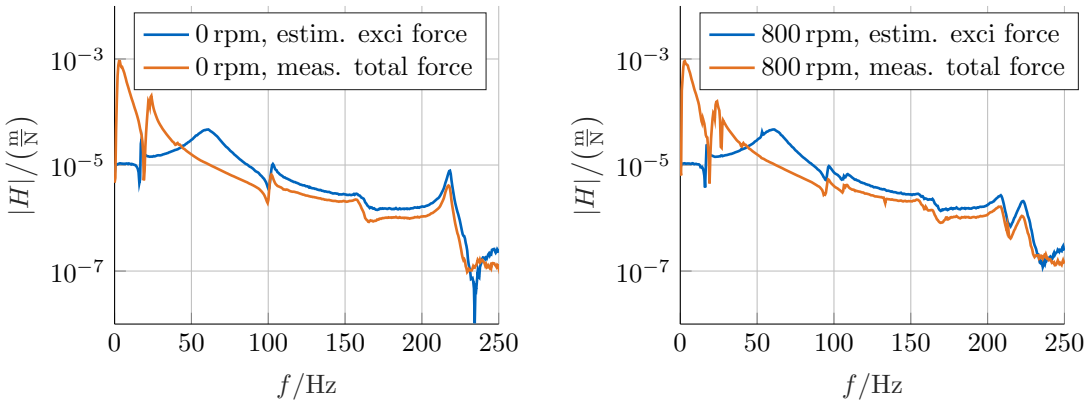

Figure 9: Comparison of the experimentally determined FRFs.

5 Summary

This contribution shows, that it is possible to measure the free FRF of a rotor and the supported system's FRF in a single measurement run using AMBs with multiple input signals. Measurement of the FRF of a rotating rotor without bearing influence could not be done using usual impact hammer FRF measurements.

With the force estimator, used in this contribution, the FRF amplitude cannot be accurately determined for low frequencies. For condition monitoring, the correct amplitude is not as critical as a continuous evaluation of the results. Thus, it could be shown, that FRFs using estimated forces are suitable for condition monitoring. The results are validated by comparison to a more accurate force measurement.

The availability of FRF of the free and the supported rotor during operation can further improve condition monitoring. It can be used to locate a possible fault. A fault in a bearing would show in the supported system's FRF, but not in the free rotor's FRF. A fault in a rotating component can be localized, if it can be observed in both types of FRFs.

The procedure for measuring FRFs of the rotating system can be investigated further as special problems arise for rotating systems. There exist a number of publications regarding suitable excitation signals for MIMO systems, like e.g. [13]. Most of them are not specific to rotating systems, but are considering feedback in general.

Free rotor FRFs can also be used to extend frequency-based substructuring, cf. [15], to rotating systems, which can for example be applied in experimental characterization of rotor system components (e.g. seals, journal bearings). This requires high-quality FRFs, i.e. force measurement or an improved force-model.

6 References

[1] Anders Brandt. *ABRAVIBE - A MATLAB toolbox for noise and vibration analysis*. www.abravibe.com. 2019. URL: `http://www.abravibe.com` (visited on 03/22/2019).

[2] Anders Brandt. *Noise and Vibration Analysis*. Chichester, UK: John Wiley & Sons, Ltd, Feb. 2011. ISBN: 9780470978160. DOI: `10.1002/9780470978160`.

[3] I. Bucher and D. J. Ewins. "Modal analysis and testing of rotating structures". In: *Philosophical Transactions of the Royal Society A: Mathematical, Physical and Engineering Sciences* 359.1778 (2001), pp. 61–96. ISSN: 1364503X. DOI: 10.1098/rsta.2000.0714.

[4] D. J. Ewins et al. *MARS - Modal Analysis of Rotating Structures: Development of Validated Structural Dynamic Modelling and Testing Techniques for Vibration Predictions in Rotating Machinery*. Tech. rep. 1996.

[5] P. Förch et al. "Modale Analyse an rotierenden Maschinen mittels Magnetlager". In: *Schwingungen in rotierenden Maschinen III*. Ed. by H. Irretier and R. Nordmann. Springer, 1995, pp. 245–254. DOI: 10.1007/978-3-322-83807-0_24.

[6] Conrad Gähler, Manuel Mohler, and Raoul Herzog. "Multivariable identification of active magnetic bearing systems". In: *JSME International Journal, Series C: Mechanical Systems, Machine Elements and Manufacturing* 40.4 (1997), pp. 548–592.

[7] *GitHub: AMrotor - A MATLAB toolbox for the Simulation of Rotating Machinery*. 2021. URL: https://github.com/AppliedMechanics/AMrotor (visited on 05/20/2021).

[8] Michael Kreutz et al. "Modaler Modellabgleich eines Rotors in Magnetlagern". In: *Sechste IFToMM D-A-CH Konferenz*. Lienz, Österreich, 2020. DOI: 10.17185/duepublico/71192.

[9] J Maierhofer et al. "AMrotor - A MATLAB ® Toolbox for the Simulation of Rotating Machinery". In: *12th International Conference on Vibrations in Rotating Machinery*. Ed. by Institute of Mechanical Engineers. Liverpool: CRC Press, Oct. 2020. DOI: 10.1201/9781003132639.

[10] Johannes Maierhofer et al. "Modellbasiertes Monitoring an magnetgelagerten Rotoren". In: *SIRM 2017* (2017).

[11] Johannes Maierhofer et al. "Progress in Calibrating Active Magnetic Bearings with Numerical and Experimental Approaches". In: *Mechanisms and Machine Science*. Vol. 63. 2018, pp. 249–261. ISBN: 9783319992723. DOI: 10.1007/978-3-319-99272-3_18.

[12] Johannes Maierhofer et al. "Using the Dynamics of Active Magnetic Bearings to perform an experimental Modal Analysis of a Rotor System". In: *SIRM 2019*. February. 2019. DOI: 10.13140/RG.2.2.26743.16809.

[13] Steven Pauwels et al. "A new MIMO sine testing technique for accelerated, high quality FRF measurements". In: *Conference Proceedings of the Society for Experimental Mechanics Series* (2006). ISSN: 21915644.

[14] Gerhard Schweitzer. "Applications and research topics for active magnetic bearings". In: *IUTAM-Symposium on Emerging Trends in Rotor Dynamics*. Vol. 25. 2009. ISBN: 9789400700192. DOI: 10.1007/978-94-007-0020-8-23.

[15] Maarten V. van der Seijs, Dennis de Klerk, and Daniel J. Rixen. "General framework for transfer path analysis: History, theory and classification of techniques". In: *Mechanical Systems and Signal Processing* 68-69 (2016), pp. 217–244. ISSN: 10961216. DOI: 10.1016/j.ymssp.2015.08.004. URL: http://dx.doi.org/10.1016/j.ymssp.2015.08.004.

[16] Thomas Thuemmel et al. "Rotor Orbits at Operation Speed and Model-Based Diagnosis of Multiple Errors". In: *Proceedings of the 10th International Conference on Rotor Dynamics – IFToMM*. Springer International Publishing, 2019, pp. 222–237. ISBN: 9783319992686. DOI: 10.1007/978-3-319-99268-6_16. URL: http://link.springer.com/10.1007/978-3-319-99268-6%7B%5C_%7D16.